

The neutron-proton mass difference

Simone Romiti^{a,b,*}

^a*Dipartimento di Matematica e Fisica, Università degli Studi Roma Tre, Rome, Italy*

^b*Istituto Nazionale di Fisica Nucleare, Sezione di Roma Tre, Rome, Italy*

E-mail: simone.romiti@uniroma3.it

We present a lattice calculation of the mass difference between neutron and proton, for which we find $M_n - M_p = 1.73(69)$ MeV. This is obtained at 1st order in the QED coupling α_{EM} and in the mass difference between u and d quarks $\frac{m_d - m_u}{\Lambda_{QCD}}$. We adopt a purely hadronic scheme to renormalize the theory and provide a prescription to separate the QED and strong IB contributions. The simulation is carried out using the ETMC gauge configurations with $N_f = 2 + 1 + 1$ dynamical quarks. We extrapolate among 3 values of the lattice spacing and pion masses in the range $M_\pi \simeq 200 - 450$ MeV.

*The 38th International Symposium on Lattice Field Theory, LATTICE2021 26th-30th July, 2021
Zoom/Gather@Massachusetts Institute of Technology*

*Speaker

1. Introduction

Today many lattice QCD calculations have reached the $O(1\%)$ precision level [1], requiring to include the Isospin Breaking (IB) Effects. The leading terms of the latter come from the $\sim O(1\%)$ corrections of $O(\hat{\alpha}_{EM})$ (QED) and $O(\frac{\hat{m}_d - \hat{m}_u}{\Lambda_{QCD}})$ (strong IB or QCD). These can be taken into account simulating u and d quarks with different masses and including QED in the action [2, 3]. However, a convenient approach consists in expanding the path integral with respect to the isospin symmetry breaking parameters. In this setup, any observable in the full theory (QCD+QED) is the sum of its isosymmetric part and the IBEs. This philosophy is the heart of the RM123 method [4–6] used in the present work. For a given observable, the slopes with respect to the IB couplings are found using the isosymmetric gauge configurations, and the IB correction at Leading Order (LO) is a linear combination of these slopes with the appropriate charge factors and counterterms. In this work the effect of IB on the hadronic spectrum is investigated with focus on $M_n - M_p$, the mass difference between neutron and proton. We also define a scheme for the separation of strong IB and QED contributions. Though conventional, this separation provides physical intuition about the sizes of the two effects.

We use a mixed action approach in the tmQCD regularization over the $N_f = 2 + 1 + 1$ ETMC gauge configurations [7]. In QCD+QED we adopt the electroquenched approximation and neglect QCD disconnected diagrams. A purely hadronic renormalization scheme is adopted, using the masses of π s, K s and Ω^- as normalization parameters to set the scale, tune the counterterms and reach the physical point.

The results found in this work are the following. We obtain $M_n - M_p = 1.73(69)$ MeV , $(M_n - M_p)^{(QED)} = -1.16(25)$ MeV and $(M_n - M_p)^{(QCD)} = 3.10(59)$ MeV . We also get a prediction for the masses of nucleons, $M_n = 0.961(20)$ GeV , $M_p = 0.959(20)$ GeV and for the πN sigma term $\sigma_{\pi N} = 43.2(1.4)$ MeV . The uncertainties are only statistical and obtained using the jackknife resampling technique.

The paper is organized as follows. In sec. (2) we briefly recap the main features of the RM123 method and set our notation for the IBEs. In sec. (3) we discuss the tuning of counterterms and give our prescription for the separation between strong IB and QED. In sec. (4) and (5) we respectively give the details of the simulations and of the analysis for the above observables. Finally in sec. (6) we give our summary and outlooks.

2. QCD+QED at LO

In the continuum, the QCD+QED Lagrangian \mathcal{L} can be written as:

$$\mathcal{L} = \mathcal{L}_0 - \Delta m_{ud} \bar{q} \tau_3 q + e A_\mu \bar{q} \gamma_\mu Q q \quad . \quad (1)$$

The first term, \mathcal{L}_0 , is symmetric under $SU(2)_I$ (isoQCD theory) and chargeless under $U(1)_{EM}$, while the rest are isospin breaking terms. We write $m_u = m_{ud} - \Delta m_{ud}$, $m_d = m_{ud} + \Delta m_{ud}$. and denote the up-down doublet with $q = (u, d)^T$. τ_3 is the third Pauli matrix and $Q = \frac{\tau_3}{2} + \frac{1}{6}$. At LO in IB we expand the path integral in e^2 and Δm_{ud} (including $O(e^2)$ counterterms for the divergences of QED diagrams [8]). The fine structure constant $\hat{\alpha}_{EM}$ renormalizes at higher orders with respect to our expansion, and we can safely use the value $\alpha_{EM} = e^2/(4\pi) = 1/137.035999084$ from [9].

On the lattice we use a mixed action approach as in [6]. This leads to the presence of counterterms for both the physical and critical masses, whose tuning is discussed in sec. (3). The LIBE in a generic hadronic mass can then be written as:

$$\Delta M_H = \left[e^2 \bar{\Delta}^{\text{EM}} + \sum_f a \Delta m_f^{cr} \bar{\Delta}_f^{\text{C}} + \sum_f a \Delta m_f \bar{\Delta}_f^{\text{M}} \right] M_H \quad , \quad (2)$$

where the $\bar{\Delta}^{\text{EM}}$ and $\bar{\Delta}_f^x$ ($x = \text{C}, \text{M}$) (for a flavor f) represent the slopes induced by the coupling in front of them. Note that at the order we are working, these can be evaluated in the isosymmetric theory. The slopes can be found individually from the corresponding corrections $\bar{\Delta}^x$ in those euclidean correlators whose isoQCD ground state has mass $M_H^{(0)}$. In fact for large times $C_H(t) \sim e^{-M_H t}$, and it's easy to show that the mass slope's effective curve is given by:

$$\bar{\Delta}^x M_H = -\partial_t \left[\frac{\bar{\Delta}^x C_H(t)}{C_H^{(0)}(t)} \right] \quad , \quad (3)$$

where $\partial_t f(t) = f(t+1) - f(t)$ (in lattice units). At finite time extent this formula is valid in absence of backward signals, i.e. for baryonic correlators with definite parity [10, 11]. In mesonic correlators however each forward signal is paired with a backward one, and the above formula gets slightly modified [6]. In this work we extract the mass slopes from a fit to a constant of these effective curves in their plateau intervals. In (2.1) are shown the expressions of the mass corrections in terms of Feynman diagrams.

We conclude this section saying that QED is introduced in a non-compact way [2], i.e. generating the photon field A_μ instead on the gauge link variables $E_\mu^{(f)} = \exp(iq_f A_\mu)$, and regularizing the infrared divergence in the photon propagator using the QED_L prescription [12], i.e. removing the $\vec{k} = 0$ mode. QED on a torus $T \times L^3$ introduces Finite Volume Effects (FVEs) in the hadronic spectrum, with polynomial behavior in $1/L$ [3, 13–15], and the QED mass correction of an hadron obeys the following asymptotic formula:

$$\Delta M(T, L) \xrightarrow{T, L \rightarrow \infty} \Delta M(\infty) - Q^2 \alpha_{EM} \left[\frac{\kappa}{2ML} \left(1 + \frac{2}{ML} \right) \right] + O\left(\frac{\alpha_{EM}}{L^3}\right) \quad . \quad (4)$$

$\kappa \approx 2.837297$, Q is the charge of the hadron in units of e and the M in the denominators can be set equal to $M(\infty)$ at this order in α_{EM} . The terms $\sim 1/L$ and $1/L^2$ are universal, namely depend only on the electric charge and mass of the hadron, with spin and structure-dependent terms starting only at higher orders. At fixed ensemble, we use this property to remove these universal FVEs from the mass corrections caused by the combination of diagrams coming from the interaction with the electromagnetic field (EM).

2.1 LIBEs in the hadronic spectrum

The LIBEs in the hadronic spectrum can be drawn from Feynman diagrams. For mesons the explicit expressions are provided in [6]. For baryons the drawing convention is analogous to [4]:

$$\bar{\Delta}^M C_N^{(1)} = - \text{[diagram 1]} + \text{[diagram 2]} , \dots , \quad (5)$$

$$\bar{\Delta}^C C_N^{(1)} = - \text{[diagram 1]} + \text{[diagram 2]} , \dots , \quad (6)$$

$$\bar{\Delta}^{\text{self}} C_N^{(1)} = - \text{[diagram 1]} - \text{[diagram 2]} + \text{[diagram 3]} + \text{[diagram 4]} , \dots , \quad (7)$$

$$\bar{\Delta}^{\text{exch}} C_N^{(1)} = - \text{[diagram 1]} + \text{[diagram 2]} , \dots , \quad (8)$$

$$\bar{\Delta}^{\text{loop}} C_N^{(1f)} = - \text{[diagram 1]} + \text{[diagram 2]} , \dots . \quad (9)$$

The dots “...” are a shorthand to denote the other diagrams trivially obtained considering the insertions on the other legs. The index $i = 1, 2, 3$ in $\bar{\Delta}^x C_N^{(i)}$ corresponds to the quark propagator with the insertion of the current generating the slope (except for $\bar{\Delta}^{\text{exch}} C_N^{(i)}$, where i denotes the leg unaffected by the photon exchange). The \otimes and \otimes are the insertions of the scalar and pseudoscalar currents respectively. For the Ω^- it's akin, differing for flavor content, spin 3/2 projection, and with a factor 2 in front of the diagrams with crossed quark legs. From the above equations we define the ratios $\mathcal{R}_i^x = -\partial_t [\bar{\Delta}^x C_N^{(i)} / C_N^{(0)}]$ for $x \in \{M, C, \text{self}, \text{exch}\}$ and $\mathcal{R}_{if}^{\text{loop}} = -\partial_t [\bar{\Delta}^x C_N^{(if)} / C_N^{(0)}]$, where $\mathcal{R} = N, \Omega$. The LIBEs in the nucleon doublet then assume the following form (see eq. (3)):

$$\begin{aligned} \Delta M_n = & -\Delta m_u N_1^M - \Delta m_d N_2^M - \Delta m_d N_3^M + \Delta m_u^{(cr)} N_1^C + \Delta m_d^{(cr)} N_2^C + \Delta m_d^{(cr)} N_3^C \\ & + q_u^2 N_1^{\text{self}} + q_d^2 N_2^{\text{self}} + q_d^2 N_3^{\text{self}} + q_u q_d N_3^{\text{exch}} + q_u q_d N_2^{\text{exch}} + q_d^2 N_1^{\text{exch}} \\ & + \sum_{f \in (\text{sea})} q_f \left[q_u N_{1f}^{\text{loop}} + q_d N_{2f}^{\text{loop}} + q_d N_{3f}^{\text{loop}} \right] + [\text{isosymm. vac. pol. diag.}] , \end{aligned} \quad (10)$$

and

$$\begin{aligned} \Delta M_p = & -\Delta m_d N_1^M - \Delta m_u N_2^M - \Delta m_u N_3^M + \Delta m_d^{(cr)} N_1^C + \Delta m_u^{(cr)} N_2^C + \Delta m_u^{(cr)} N_3^C \\ & + q_d^2 N_1^{\text{self}} + q_u^2 N_2^{\text{self}} + q_u^2 N_3^{\text{self}} + q_d q_u N_3^{\text{exch}} + q_d q_u N_2^{\text{exch}} + q_u^2 N_1^{\text{exch}} \\ & + \sum_{f \in (\text{sea})} q_f \left[q_d N_{1f}^{\text{loop}} + q_u N_{2f}^{\text{loop}} + q_u N_{3f}^{\text{loop}} \right] + [\text{isosymm. vac. pol. diag.}] . \end{aligned} \quad (11)$$

The neutron-proton mass difference at LO is:

$$\begin{aligned} M_n - M_p = & -2\Delta m_{ud} [N_1^M - N_2^M - N_3^M] + 2\Delta m_{ud}^{(cr)} [N_1^C - N_2^C - N_3^C] \\ & + (q_u^2 - q_d^2) [N_1^{\text{self}} - N_2^{\text{self}} - N_3^{\text{self}} - N_1^{\text{exch}}] \\ & + \sum_{f \in (\text{sea})} q_f (q_u - q_d) \left[N_{1f}^{\text{loop}} - N_{2f}^{\text{loop}} - N_{3f}^{\text{loop}} \right] . \end{aligned} \quad (12)$$

Finally the IB correction to M_{Ω^-} is:

$$\begin{aligned} \Delta M_{\Omega^-} = & -\Delta m_s [\Omega_1^M + \Omega_2^M + \Omega_3^M] + \Delta m_s^{(cr)} [\Omega_1^C + \Omega_2^C + \Omega_3^C] \\ & + q_s^2 [\Omega_1^{\text{self}} + \Omega_2^{\text{self}} + \Omega_3^{\text{self}} + \Omega_3^{\text{exch}} + \Omega_2^{\text{exch}} + \Omega_1^{\text{exch}}] \\ & + \sum_{f \in (\text{sea})} q_f q_s \left[\Omega_{1f}^{\text{loop}} + \Omega_{2f}^{\text{loop}} + \Omega_{3f}^{\text{loop}} \right] + [\text{isosymm. vac. pol. diag.}] \quad . \end{aligned} \quad (13)$$

In this work we neglect the (disconnected) isosymmetric vacuum polarization diagrams, and work in the electroquenched approximation: sea quarks are neutral with respect to the photon field, i.e. all diagrams with photons attached to quark loops vanish. This gives the numerical advantage of not having to evaluate the LIBEs also in the sea quark determinant.

3. Counterterms and separation between QCD and QED

In tmQCD the inclusion of QED introduces counterterms to the critical and physical masses. In this work the former are tuned from the infinite volume limit of the PCAC Ward Identity (WI) integrated over the 3 spatial directions. Our values of am_0^{cr} have been already tuned to get maximal twist in absence of IB [16]. Here we require to preserve maximal twist (and hence the $O(a)$ improvement [17]) also at $O(e^2)$. Therefore, for each flavor, we find the bare counterterms $a\Delta m_f$ from a fit to a constant of the following condition in its plateau region:

$$0 = \Delta m_f^{PCAC}(t) = \Delta^{\text{EMC}} \left(\frac{\partial_t \langle A_4^a(t) P^a(0) \rangle}{\langle P^a(t) P^a(0) \rangle} \right) \quad , \quad (14)$$

where $P^a = \sum_{\vec{x}} \bar{\chi}_f(x) \gamma^5 \frac{\tau^a}{2} \chi_f(x)$ and $A_\mu^a = \sum_{\vec{x}} \bar{\chi}_f(x) \gamma_\mu \gamma^5 \frac{\tau^a}{2} \chi_f(x)$ in the twisted basis. The tuning is done at fixed ensemble, and we sum the EM effective correction with the effect of critical mass counterterms (C) getting the variation ΔM^{EMC} .

The physical mass counterterms are then tuned as follows. We define the physical point of both isoQCD and QCD+QED from the ratios:

$$r_s = \frac{2(M_{K^+}^2 + M_{K^0}^2) - (M_{\pi^+}^2 + M_{\pi^0}^2)}{2M_{\Omega^-}^2} \quad , \quad r_\ell = \frac{M_{\pi^+}^2 + M_{\pi^0}^2}{2M_{\Omega^-}^2} \quad , \quad r_p = \frac{M_{K^+}^2}{M_{\Omega^-}^2} \quad , \quad (15)$$

imposing $r_s = r_s^{(exp)}$, $r_\ell = r_\ell^{(exp)}$ and $r_p = r_p^{(exp)}$. This also implies, by definition, that their total IB corrections vanishes. Expanding according to the LO corrections to the masses (see sec. (2.1)), we have:

$$r_i = r_i^{(0)} + \sum_{f \in (u,d,s)} a\Delta m_f \bar{\Delta}_f^M r_i + \Delta r_i^{\text{EMC}} \quad (i = s, \ell, p) \quad , \quad (16)$$

so that at our physical point, where $r_i = r_i^{(0)}$, the solution to the above system defines the counterterms as:

$$\begin{bmatrix} a\Delta m_u \\ a\Delta m_d \\ a\Delta m_s \end{bmatrix} = - \begin{bmatrix} \bar{\Delta}_u^M r_s & \bar{\Delta}_d^M r_s & \bar{\Delta}_s^M r_s \\ \bar{\Delta}_u^M r_\ell & \bar{\Delta}_d^M r_\ell & \bar{\Delta}_s^M r_\ell \\ \bar{\Delta}_u^M r_p & \bar{\Delta}_d^M r_p & \bar{\Delta}_s^M r_p \end{bmatrix}^{-1} \begin{bmatrix} \Delta r_s^{\text{EMC}} \\ \Delta r_\ell^{\text{EMC}} \\ \Delta r_p^{\text{EMC}} \end{bmatrix} \quad . \quad (17)$$

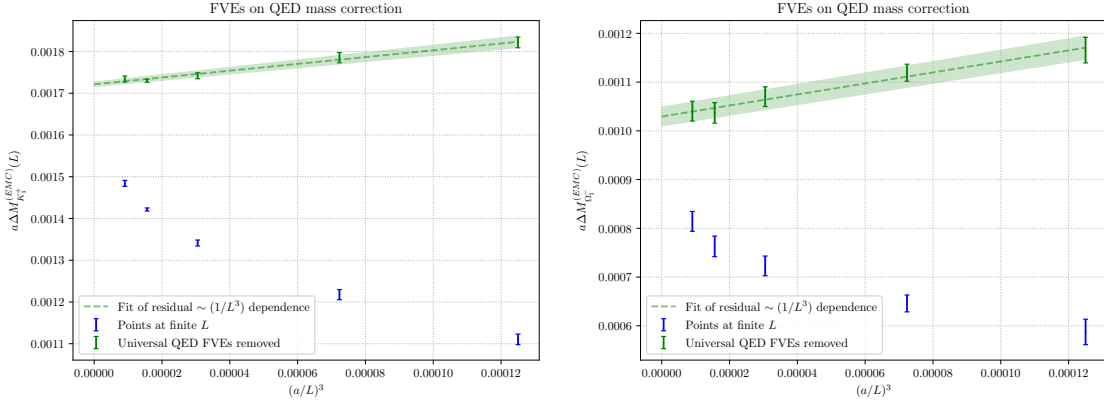


Figure 1: EMC corrections for the K^+ and Ω^- obtained from the 1st of the 2 simulated values of am_s , for the A40.XX ensembles. The blue points are the EMC corrections in lattice units at finite volume. The green points are the values after the correction of the universal QED FVEs. The green band is a fit of the latter with an ansatz of the form $A + B \left(\frac{a}{L}\right)^3$, with A and B free parameters of the fit.

These equations give the counterterms at the isoQCD physical point of am_s and am_ℓ (or equivalently of r_s and r_ℓ). In the analysis however the $a\Delta m_f$ are found at fixed simulated light quark mass, after the interpolation of the slopes among the 2 values of am_s to the physical point of r_s . These $a\Delta m_f$ are used to evaluate the other observables, which are then extrapolated to $L \rightarrow \infty$, $a \rightarrow 0$ and $r_\ell = r_\ell^{(exp)}$ over all the ensembles. For each observable O this is just an extrapolation in separate steps, done on the slice $r_s = r_s^{(exp)}$ of the hyper-surface $O(r_s, r_\ell, L, a)$.

We remark that, after the subtraction of the universal $1/L$ and $1/L^2$ corrections of eq. (4), these Δm_f contain residual $O(\alpha_{EM}/L^3)$ FVEs from QED. These have been removed before the tuning from the EMC corrections. Fig. (1) shows the behavior of 2 of our EMC corrections using the A40.XX ensembles, which differ only for the volume.

We can now provide a prescription for the separation of strong IB (QCD) and QED. Here we implement the separation as in [6], namely we write:

$$\Delta m_{ud} = \frac{m_d - m_u}{2} = \Delta m_{ud}^{(QCD)} + \Delta m_{ud}^{(QED)} = \frac{\Delta \hat{m}_{ud}}{Z_P^{(0)}} + \frac{(q_d^2 - q_u^2)}{32\pi^2} [6 \log(a\mu) - 22.595] m_\ell^{(0)} \quad . \quad (18)$$

With the notation of sec. (2.1), the contributions to the mass difference $M_n - M_p$ then read:

$$\begin{aligned} (M_n - M_p)^{(QCD)} &= -2\Delta m_{ud}^{(QCD)} [\mathcal{N}_1^M - \mathcal{N}_2^M - \mathcal{N}_3^M] \quad , \quad (19) \\ (M_n - M_p)^{(QED)} &= -2\Delta m_{ud}^{(QED)} [\mathcal{N}_1^M - \mathcal{N}_2^M - \mathcal{N}_3^M] + 2\Delta m_{ud}^{(cr)} [\mathcal{N}_1^C - \mathcal{N}_2^C - \mathcal{N}_3^C] \\ &\quad + (q_u^2 - q_d^2) [\mathcal{N}_1^{\text{self}} - \mathcal{N}_2^{\text{self}} - \mathcal{N}_3^{\text{self}} - \mathcal{N}_{23}^{\text{exch}}] \\ &\quad + \sum_{f \in (\text{sea})} q_f (q_u - q_d) \left[\mathcal{N}_{1f}^{\text{loop}} - \mathcal{N}_{2f}^{\text{loop}} - \mathcal{N}_{3f}^{\text{loop}} \right] \quad . \quad (20) \end{aligned}$$

The physical interpretation is that the neutron tends to be heavier because $m_d > m_u$. The u however has a bigger electric charge, giving an higher electromagnetic self energy to the proton. In

Ensemble	β	V/a^4	$am_{sea} = am_\ell$	am_s	am_σ	am_δ	κ	N_{cfg}
A30.32	1.90	$32^3 \times 64$	0.0030	0.0242, 0.0261	0.15	0.19	0.163272	150
A40.32			0.0040				0.163270	150
A50.32			0.0050				0.163267	150
A40.20	1.90	$20^3 \times 48$	0.0040	0.0242, 0.0261	0.15	0.19	0.163270	150
A40.24	1.90	$24^3 \times 48$	0.0040	0.0242, 0.0261	0.15	0.19	0.163270	150
A60.24			0.0060				0.163265	150
A80.24			0.0080				0.163255	150
A100.24			0.0100				0.163260	150
A40.48	1.90	$48^3 \times 96$	0.0040	0.0242, 0.0261	0.15	0.19	0.163270	90
A40.40	1.90	$40^3 \times 80$	0.0040	0.0242, 0.0261	0.15	0.19	0.163270	150
B25.32	1.95	$32^3 \times 64$	0.0025	0.0216, 0.0230	0.135	0.170	0.1612420	150
B35.32			0.0035				0.1612400	150
B55.32			0.0055				0.1612360	150
B75.32			0.0075				0.1612320	75
B85.24	1.95	$24^3 \times 48$	0.0085	0.0216, 0.0230	0.135	0.170	0.1612312	150
D15.48	2.10	$48^3 \times 96$	0.0015	0.0176, 0.0186	0.12	0.1385	0.156361	90
D20.48			0.0020				0.156357	90
D30.48			0.0030				0.156355	90

Table 1: Parameters of the ensembles used in this work. The space-time volume is reported in the format $L^3 \times T$. The bare values for β , sea and valence quark masses and hopping parameter κ are reported. am_σ and am_δ are the parameters which determine the renormalized strange and charm sea quark masses according to eq. (9) of [7]. In the rightmost column there are the number of analyzed gauge configurations.

nature it happens that these effects are of the same order of magnitude, canceling almost exactly and leaving a small mass difference, $O(1 \text{ MeV})$, compared to their masses, $O(1 \text{ GeV})$. We conclude remarking, however, that the above separation is a matter of prescription, since it's arbitrary to choose which finite terms go in the divergent term $\Delta m_{ud}^{(QED)}$.

4. Details of simulation and analysis

Our correlators are evaluated over the $N_f = 2 + 1 + 1$ ETMC gauge configurations [7] with twisted mass quarks at maximal twist. We adopt a unitary setup in the light sector, and a mixed action approach for the strange and charm quarks which in the valence are regularized as Osterwalder-Seyler fermions [18]. In tab. (1) are reported the ensembles details. The statistical uncertainty on our observables was propagated using the jackknife re-sampling technique with 15 jackknives for each ensemble. Gaussian smearing was applied to quark fields according to [4], with the parameter α_g optimized as in [19]. Some numerical testing lead us to the choice of $n_g = 50$ steps on the source of our correlators, as an appropriate middle ground for a soon plateau and moderate noise in the signal. In order to reduce the noise in our correlator, we used 16 stochastic sources [20] for the numerical inversion of the Dirac operator, compatibly with our computational resources.

The isosymmetric limit of hadronic masses M_H are found from the large time behavior of $\vec{p} = \vec{0}$ correlators with $M_H^{(0)}$ as the ground state. These values are found from a fit to a constant of the effective mass curves [17] in their plateau intervals ¹, and we do the same also for the effective slopes curves (see sec. (2)).

Our lattice ensembles are not at the physical point, requiring to extrapolate among the ensembles. This is done in an hadronic scheme, in terms of the ratios defined in eq. (15). M_{Ω^-} , $(M_{\pi^+}^2 + M_{\pi^0}^2)$, $M_{K^+}^2$ and $M_{K^0}^2$ are used to tune the parameters a , am_u , am_d and am_s , with the counterterms $a\Delta m_f$ defined at the isoQCD physical point (see sec. (3)). The lattice spacings $a_{\beta(i)} = 0.1011(10), 0.09029(77), 0.06834(63)$ fm at $\beta = 1.90, 1.95, 2.10$ respectively, are found from the extrapolation of aM_{Ω^-} among the ensembles, whose values are fitted with the following polynomial ansatz:

$$(aM_{\Omega^-})_i(L, r_\ell) = a_{\beta(i)} M_{\Omega^-}^{(exp)} \left[1 + c_L \frac{\alpha_{EM}}{L^3} + c_\ell \Delta r_\ell + c_\ell^{(2)} \Delta r_\ell^2 \right] \quad . \quad (21)$$

$\Delta r_\ell = r_\ell - r_\ell^{exp}$ and $c_L, c_\ell, c_\ell^{(2)}$ and the $a_{\beta(i)}$ ($i = 1, 2, 3$) are free parameters of the fit. The numerically leading FVE is taken into account with the $\sim 1/L^3$ term, coming from the residual QED FVEs in $a\Delta m_s$ and $\Delta M_{\Omega^-}^{EMC}$.

Each observable is extrapolated among 2 values of am_s and the am_ℓ of tab. (1) to the isoQCD physical point in terms of the ratios r_s and r_ℓ of eq. (15). FVEs are fitted using asymptotic formulas from ChPT (isoQCD FVEs) [22–24] and QED at finite volume [3, 13–15], while discretization effects are included with $O(a^2)$ terms in virtue of the $O(a)$ improvement provided by maximal twist.

5. Nucleons spectrum

The masses of nucleons are found for each ensemble, summing the isosymmetric part M_N to the IB corrections given in eqs. (10) and (11). We fit M_n and M_p according to the following ansatz inspired by ChPT [25]:

$$M_{n/p}(L, r_\ell, a) = A_{n/p} \left[1 + \alpha_{EM} \frac{c_3^{(n/p)}}{L^3} + c_a^{(n/p)} a^2 + c_\ell^{(n/p)} r_\ell + c_{3/2}^{(n/p)} r_\ell^{3/2} \right] \quad , \quad (22)$$

where the coefficients $A_{n/p}, \dots$ are free parameters of the fit. Similarly, The mass difference $M_n - M_p$ is found from eq. (12), and fitted with a simple polynomial ansatz:

$$(M_n - M_p)(L, r_\ell, a) = A \left[1 + \alpha_{EM} \frac{c_3}{L^3} + c_a a^2 + c_\ell r_\ell \right] \quad , \quad (23)$$

where the coefficients A, \dots , are free parameters of the fit. We account for the volume dependence with an $O(\alpha_{EM}/L^3)$ term, arising from the structure-dependence and the residual dependence in physical mass counterterms. In both cases higher orders of $1/L$ and the isoQCD FVEs are found to be numerically negligible at our level of precision.

In fig. (2), we show the plot of the extrapolation for the average mass $M_{np} = (M_n + M_p)/2$ and $M_n - M_p$. Our predictions are the following, with the uncertainties being statistical. We find

¹As a consistency check, we also verified the results with the leading exponential fit and the ODE method [21].

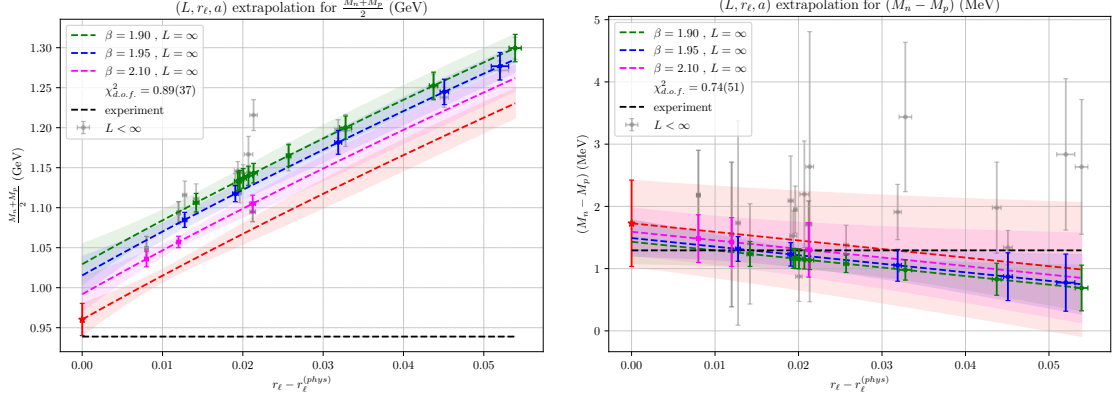


Figure 2: Extrapolation of $(M_n + M_p)/2$ (left panel) and $M_n - M_p$ (right panel). Grey points are the values at finite volume. The colored points and lines correspond to the limit $L \rightarrow \infty$. The red curves are the continuum and infinite volume limits. The final predictions at $r_\ell = r_\ell^{(\text{phys})}$ are marked on the left. The horizontal black lines are the experimental values.

[26]:

$$M_n = 0.961(20) \text{ GeV} \quad [0.9395654133(58) \text{ GeV}]_{\text{exp}} \quad , \quad (24)$$

$$M_p = 0.959(20) \text{ GeV} \quad [0.9382720813(58) \text{ GeV}]_{\text{exp}} \quad , \quad (25)$$

and

$$M_n - M_p = 1.73(69) \text{ MeV} \quad [1.29333205(51) \text{ MeV}]_{\text{exp}} \quad . \quad (26)$$

Finally, we extrapolate the two contributions $(M_n - M_p)^{(QCD)}$ and $(M_n - M_p)^{(QED)}$ of eqs. (19) and (20), using the same functional form of eq. (23). We find:

$$(M_n - M_p)^{(QCD)} = 3.10(59) \text{ MeV} \quad , \quad (27)$$

$$(M_n - M_p)^{(QED)} = -1.16(25) \text{ MeV} \quad . \quad (28)$$

In fig. (3) are shown the plots of the extrapolations for these two quantities.

6. Summary and outlook

In this work we've discussed the inclusion of LIBEs effects in the nucleons spectrum, finding their masses and the difference $M_n - M_p$.

The $O(\alpha_{EM})$ and $O(\frac{\hat{m}_d - \hat{m}_u}{\Lambda_{QCD}})$ corrections have been taken into account using the RM123 method. Critical masses were fixed by the PCAC Ward Identity in order to preserve the maximal twist condition at LO. The physical masses are tuned using an hadronic scheme and the lattice spacing is fixed through M_{Ω^-} .

We worked in the electroquenched approximation and neglected QCD disconnected diagrams. At our level of precision these are expected to be suppressed, giving a negligible contribution. This assumption is confirmed by the consistency of our results with the experimental values. For

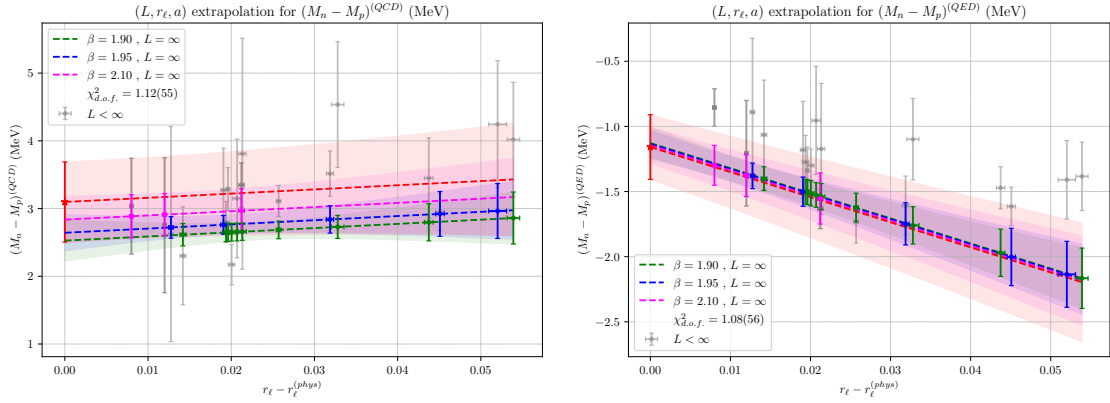


Figure 3: The same as fig. (2) but for $(M_n - M_p)^{(QCD)}$ and $(M_n - M_p)^{(QED)}$.

a sequent work we aim at including these diagrams, whose effects can be known only by direct evaluation, and provide an estimate of the various sources of systematic errors.

In the future we also aim at applying the RM123 method to neutron β decay, which has phase space size given by $M_n - M_p$. A good prediction of this quantity is the preliminary step to face up to the radiative corrections in the decay width, from which one could improve the determination of radiative corrections in the CKM matrix element V_{ud} .

7. Acknowledgements

The numerical simulations were carried out on the CINECA Tier-0 supercomputer MARCONI. I gratefully acknowledge the CPU time provided by PRACE under the project Pra10-2693 ‘‘QED corrections to meson decay rates in Lattice QCD’’ and by CINECA under the specific initiative INFN-LQCD123. I am also grateful to V. Lubicz, S. Simula, F. Sanfilippo, G. Martinelli and C. Tarantino for their support and fruitful discussions during the evolution of this project.

References

- [1] G. Colangelo, S. Durr, A. Juttner, L. Lellouch, H. Leutwyler, V. Lubicz et al., *Review of lattice results concerning low-energy particle physics*, *The European Physical Journal C* **71** (2011) 1.
- [2] A. Duncan, E. Eichten and H. Thacker, *Electromagnetic splittings and light quark masses in lattice qcd*, *Physical review letters* **76** (1996) 3894.
- [3] S. Borsanyi, S. Durr, Z. Fodor, C. Hoelbling, S. Katz, S. Krieg et al., *Ab initio calculation of the neutron-proton mass difference*, *Science* **347** (2015) 1452.
- [4] G. De Divitiis, P. Dimopoulos, R. Frezzotti, V. Lubicz, G. Martinelli, R. Petronzio et al., *Isospin breaking effects due to the up-down mass difference in lattice qcd*, *Journal of High Energy Physics* **2012** (2012) 1.

- [5] N. Tantalo, *Isospin breaking effects on the lattice*, 2013.
- [6] RM123 COLLABORATION collaboration, *Leading isospin breaking effects on the lattice*, *Phys. Rev. D* **87** (2013) 114505.
- [7] N. Carrasco, A. Deuzeman, P. Dimopoulos, R. Frezzotti, V. Giménez, G. Herdoiza et al., *Up, down, strange and charm quark masses with $nf=2+1+1$ twisted mass lattice qcd*, *Nuclear Physics B* **887** (2014) 19.
- [8] M.E. Peskin and D.V. Schroeder, *An introduction to quantum field theory (boulder, co)*, 1995.
- [9] P.D. Group, P.A. Zyla, R.M. Barnett, J. Beringer, O. Dahl, D.A. Dwyer et al., *Review of Particle Physics*, *Progress of Theoretical and Experimental Physics* **2020** (2020) [<https://academic.oup.com/ptep/article-pdf/2020/8/083C01/34673722/ptaa104.pdf>].
- [10] S. Sasaki, *N^* spectrum in lattice qcd*, 2000.
- [11] F.X. Lee and D.B. Leinweber, *Negative-parity baryon spectroscopy*, *Nuclear Physics B - Proceedings Supplements* **73** (1999) 258.
- [12] D. Giusti, V. Lubicz, C. Tarantino, G. Martinelli, F. Sanfilippo, S. Simula et al., *Leading isospin-breaking corrections to pion, kaon, and charmed-meson masses with twisted-mass fermions*, *Physical Review D* **95** (2017) 114504.
- [13] S. Uno and M. Hayakawa, *QED in Finite Volume and Finite Size Scaling Effect on Electromagnetic Properties of Hadrons*, *Progress of Theoretical Physics* **120** (2008) 413 [<https://academic.oup.com/ptp/article-pdf/120/3/413/5203205/120-3-413.pdf>].
- [14] Z. Davoudi and M.J. Savage, *Finite-volume electromagnetic corrections to the masses of mesons, baryons, and nuclei*, *Physical Review D* **90** (2014) 054503.
- [15] Z. Fodor, C. Hoelbling, S. Katz, L. Lellouch, A. Portelli, K. Szabo et al., *Quantum electrodynamics in finite volume and nonrelativistic effective field theories*, *Physics Letters B* **755** (2016) 245.
- [16] R. Baron, P. Boucaud, P. Dimopoulos, R. Frezzotti, D. Palao, G. Rossi et al., *Light meson physics from maximally twisted mass lattice qcd*, *Journal of High Energy Physics* **2010** (2010) 1.
- [17] C. Gattringer and C. Lang, *Quantum chromodynamics on the lattice: an introductory presentation*, vol. 788, Springer Science & Business Media (2009).
- [18] K. Osterwalder and E. Seiler, *Gauge field theories on a lattice*, *Annals of Physics* **110** (1978) 440.
- [19] C. Alexandrou, R. Baron, B. Blossier, M. Brinet, J. Carbonell, P. Dimopoulos et al., *Light baryon masses with dynamical twisted mass fermions*, *Physical Review D* **78** (2008) 014509.

- [20] M. Foster, C. Michael, U. collaboration et al., *Quark mass dependence of hadron masses from lattice qcd*, *Physical Review D* **59** (1999) 074503.
- [21] S. Romiti and S. Simula, *Extraction of multiple exponential signals from lattice correlation functions*, *Phys. Rev. D* **100** (2019) 054515.
- [22] G. Colangelo and S. Dürr, *The pion mass in finite volume*, *The European Physical Journal C-Particles and Fields* **33** (2004) 543.
- [23] G. Colangelo, S. Dürr and C. Haefeli, *Finite volume effects for meson masses and decay constants*, *Nuclear Physics B* **721** (2005) 136.
- [24] G. Colangelo and A. Fuhrer, *Finite volume effects for nucleon and heavy meson masses*, *Physical Review D* **82** (2010) 034506.
- [25] C. Alexandrou, R. Baron, J. Carbonell, V. Drach, P. Guichon, K. Jansen et al., *Low-lying baryon spectrum with two dynamical twisted mass fermions*, *Physical Review D* **80** (2009) 114503.
- [26] P.J. Mohr, D.B. Newell and B.N. Taylor, *CODATA Recommended Values of the Fundamental Physical Constants: 2014*, *Rev. Mod. Phys.* **88** (2016) 035009 [1507.07956].